Nanoscale Res Lett (2007) 2:303–307
DOI 10.1007/s11671-007-9066-4

NANO EXPRESS

Narrow ridge waveguide high power single mode 1.3-μm InAs/InGaAs ten-layer quantum dot lasers

Q. Cao · S. F. Yoon · C. Y. Liu · C. Y. Ngo

Received: 18 April 2007 / Accepted: 23 May 2007 / Published online: 14 June 2007

Abstract Ten-layer InAs/$In_{0.15}Ga_{0.85}As$ quantum dot (QD) laser structures have been grown using molecular beam epitaxy (MBE) on GaAs (001) substrate. Using the pulsed anodic oxidation technique, narrow (2 μm) ridge waveguide (RWG) InAs QD lasers have been fabricated. Under continuous wave operation, the InAs QD laser ($2 \times 2{,}000$ μm^2) delivered total output power of up to 272.6 mW at 10 °C at 1.3 μm. Under pulsed operation, where the device heating is greatly minimized, the InAs QD laser ($2 \times 2{,}000$ μm^2) delivered extremely high output power (both facets) of up to 1.22 W at 20 °C, at high external differential quantum efficiency of 96%. Far field pattern measurement of the 2-μm RWG InAs QD lasers showed single lateral mode operation.

Keywords Molecular beam epitaxy · Single lateral mode · InAs/InGaAs quantum dot · Pulsed anodic oxidation · Laser diode

Introduction

High-performance GaAs-based quantum dot (QD) lasers are of great interest due to their potential applications in advanced optical fiber communication systems [1–9]. The reduced density of states arising from the three-dimensional confinement of carriers give QDs the advantages to be able to achieve low threshold current density and high differential gain [2, 5, 6, 10]. High power, high efficiency, and temperature insensitivity have been reported for InAs QD lasers [3, 5, 6]. However, the laser performance is commonly restrained by the intrinsically low surface density (N_{QD}) of a single-layer QD structure [7]. As the achievable optical gain, which is limited by saturated gain (G^{sat}), in a single-layer QD is proportional to the surface density, i.e., $G^{sat} \propto N_{QD}$, the finite N_{QD} of the order of 10^{10} cm^{-2} in a self-assembled single-layer QD structure directly limits the available optical gain in the ground state (GS) [7, 8]. This leads to undesirable excited state (ES) lasing at high current and/or high temperature [9].

Over the last decade, it has been shown that utilization of multiple QD layers is an effective way to prevent gain saturation [3, 5–7, 9, 11–15]. Ideally, the saturation gain [6] and maximum output power increase [11] following increase in the number of QD layers. However in practice, the high strain accumulated in the multiple-layer QD active region generates defects formation, leading to degradation in the threshold current (I_{th}) and internal quantum efficiency (η_i) [6, 14]. This limits the number of stacking layers that can be incorporated into the QD active region. So far, laser structures comprising three to five QD active layers have been reported [5, 9, 11–13, 16, 17]. However, there have been relatively few reports [3, 6, 14, 15] on QD lasers emitting at 1.3 μm or above, with the number of QD active layers exceeding five.

Furthermore, single mode laser operation [12, 13, 18–20] is desirable for better device to fiber coupling efficiency in optical fiber communication systems. This could be achieved using narrow ridge waveguide (RWG) laser structure [12, 13, 15, 18–21]. There have been many studies of RWG structure in InGaAsN/GaAs QW and In(Ga)As/GaAs QD systems, where light emission at 1.3 μm is realized. High power single mode operation has been achieved in InGaAsN/GaAs QW lasers, where high

Q. Cao · S. F. Yoon (✉) · C. Y. Liu · C. Y. Ngo
School of Electrical and Electronic Engineering, Nanyang Technological University, Nanyang Avenue, Singapore 639798, Republic of Singapore
e-mail: esfyoon@ntu.edu.sg

performance in terms of light output, beam quality and high-temperature operation have been demonstrated [18–20]. Comparatively, fewer works have been reported on single mode operation in high performance In(Ga)As/GaAs QD lasers [12, 13]. It is commonly known that as the ridge width narrows, the sidewall condition plays an important role in the laser performance, where sidewall scattering/recombination [22] tends to degrade the laser performance. Undesirable lateral current spreading resulting from sidewall effects have been investigated for improving the laser structure design [22–24]. Moreover, the small lasing volume in narrow RWG lasers may increase the optical losses as result of process related scattering. Such effects may increase the threshold current density and limit high temperature operation [25]. A key factor to achieve single mode emission is narrow ridge width of the QD laser structure. To obtain strong index guiding and to suppress current spreading, careful balance between etch depth and ridge width should be accomplished [22]. Our previous works [26, 27] have shown that by optimizing the pulsed anodic oxidation (PAO) process after sidewall etching, high-performance RWG lasers with reduced lateral current spreading could be achieved.

While we have previously demonstrated [14] low transparency current density and high temperature characteristic ten-layer InAs broad area QD lasers, this paper reports the characteristics of ten-layer narrow ridge width (2 μm) InAs QD lasers. We will show results from devices with high output power of 272.6 mW (both facets) operated in continuous wave (CW) mode under GS lasing at 1.3 μm emission. Devices of dimension $2 \times 2{,}000$ μm^2 operated under pulsed mode (pulse width = 1 μs, duty cycle = 1%) showed extremely high output power of up to 610 mW per facet. The narrow RWG InAs QD lasers also emit in single lateral mode.

Experimental details

The ten-layer self-assembled InAs/InGaAs QD laser structures were grown using molecular beam epitaxy (MBE) on GaAs (100) substrates. Separate confinement layers based on 1.5-μm-thick $Al_{0.35}Ga_{0.65}As$ cladding layers doped with C and Si for p- and n-type conductivity, respectively (refer to Fig. 1a), were used. The QD active region (refer to Fig. 1b), consists of 10 layers of InAs (2.32 ML)/$In_{0.15}Ga_{0.85}As$ (5 nm) QDs separated by a 33 nm-thick GaAs spacer inserted into two $Al_{0.35}Ga_{0.65}As$ cladding layers. p-doping modulation (C: 5×10^{17} cm^{-3}) was incorporated into the 10 nm GaAs layer in the middle of each 33 nm-thick spacer between the QD rows. A 200 nm-thick P^+-GaAs cap layer was used for electrical contact. Evidence of high optical quality of the QD laser structure was obtained from photoluminescence (PL) measurements. Details from the PL study were published elsewhere [14]. GS photoluminescence up to 100 °C was demonstrated from this QD laser structure. Though both GS and first excited state (ES) transitions were observed, GS emissions remained dominant even at high excitation power and high temperature. This indicates that the QD laser structure exhibits strong luminescent efficiency without degradation in material quality even with ten QD layers [14]. Normally, QD lasers switch to the ES lasing at high temperature due to reduction of the GS gain as result of thermally activated carrier loss and increased band-filling in the ES as the GS gain becomes saturated [28]. Since GS emission was maintained in the InAs QD laser structure up to 100°C under high excitation level, this indicates the availability of high GS gain from the p-doped ten-layer InAs QD active region.

The wafer was processed into 2 μm wide RWG lasers by standard wet chemical etching using a solution of

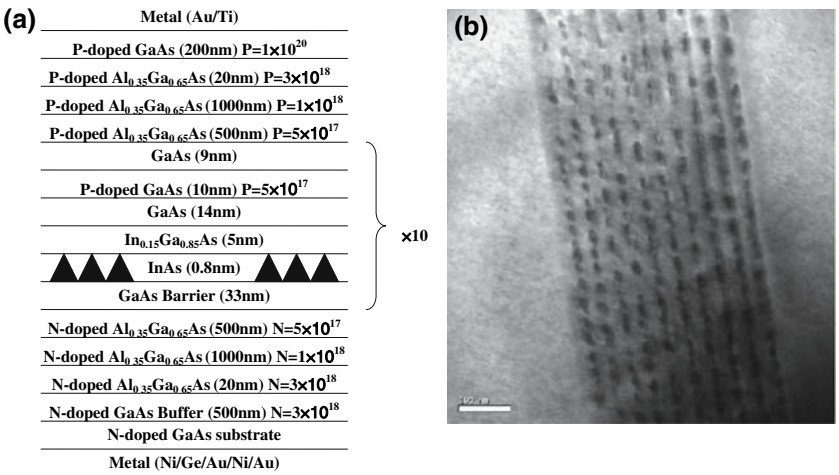

Fig. 1 (**a**) Schematic illustration of the InAs/InGaAs ten-layer QD laser structure. (**b**) TEM image of the InAs QD active region. The scale bar is 100 nm

H_3PO_4:H_2O_2:H_2O (1:1:5). Good control of the etch depth is necessary to achieve single lateral mode operation, since the refractive index step between the ridge and trench region is determined by the etch depth. Through optimization of the ridge height [27, 29], the entire p-doped layers above the QD active region outside the ridge was etched before the pulsed anodic oxidation (PAO) process. A 200 nm-thick oxide layer was formed by PAO, whose experimental setup is described in Ref. [30]. Subsequently, p-type ohmic contact layers (Ti/Au, 50/300 nm) were deposited by electron beam evaporation, while n-type ohmic contact layers (Ni/Ge/Au/Ni/Au, 5/20/100/25/300 nm) were deposited on the backside of the substrate following lapping down to ~100 μm. All samples were annealed at 410 °C for 3 min in N_2 ambient. Finally, the wafers were cleaved into laser bars of different cavity lengths (550–3,000 μm), whereas, the ridge width was kept constant for all the laser devices at w = 2 μm. The output power (P) versus injection current (I) (P–I) characteristics were measured under CW operation at 10 °C. To minimize device heating, the InAs QD lasers were also tested under pulsed operation (pulse width = 1 μs, duty cycle = 1%) at 20 °C. The far field patterns (parallel to the junction plane) of the InAs QD lasers were measured under the above mentioned pulsed conditions at 20 °C.

Results and discussion

Figure 2a shows a cross-sectional scanning electron microscopy (SEM) image of the narrow RWG laser structure investigated in this work. A stripe width of 2 μm is clearly shown and the etching was stopped right above the upper cladding layer as described previously. The oxidized AlGaAs layer (~200 nm thick) formed by PAO above the active region is observed in Fig. 2a. The oxide layer is smooth and uniform, and no signs of under-cut were observed. Meanwhile, the ten-stacked QD layers are clearly presented in Fig. 2b with better contrast.

Figure 3 shows the plot of CW output power and biasing voltage (V) as function of injection current, I taken from devices of dimension 2 × 2,000 μm^2 at 10 °C. High output power (both facets) of around 272.6 mW was obtained. The output power eventually saturated at 800 mA due to thermal rollover. However, distinct kinks were observed under high current injection, which we attribute to mode hopping caused by device heating [31], rather than current-induced ground-to-excited-state lasing transition [16]. The latter mechanism, caused by finite intraband relaxation time combined with limited density of GS in QD structures, is only significant for short-cavity devices, in which the number of available ground states for carrier relaxation is reduced [14, 17]. Furthermore, a report by Markus et al. [17] indicated that the ES threshold current is more than 10 times higher than GS threshold current for cavity length of 2,000 μm, which is not true in our case. The lasing spectrum from an InAs QD laser (50 × 5,000 μm^2) is presented in the inset of Fig. 3 for verification. The lasing wavelengths of 1,308 nm and 1,351.1 nm are obtained under the injection current of 354 mA at 25 °C and 1 A at 100 °C, respectively. It does prove GS lasing from such laser structure under high injection current level even at high temperature up to 100 °C. Based on above analysis, it is reasonable to conclude that the kink in power output is most likely caused by longitudinal mode hopping, which arises primarily due to temperature fluctuation in the laser. The heating of the laser active region by the injection current under CW operation, may cause nonlinearity in

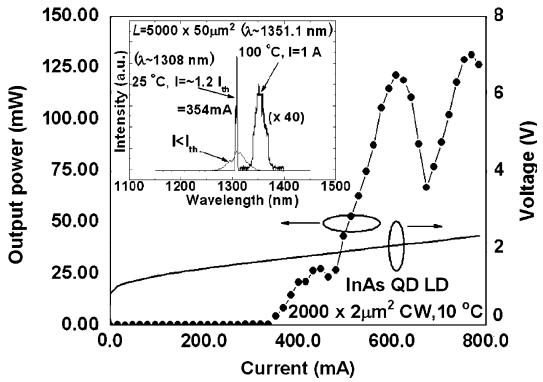

Fig. 3 P–I–V characteristics of a 2 × 2,000 μm^2 RWG InAs QD laser in CW operation. The output power is obtained from the front as-cleaved facet. Inset shows the lasing spectrum from an InAs QD laser (50 × 5,000 μm^2). The laser showed ground state lasing from 25 °C up to 100 °C with the injection current up to 1 A

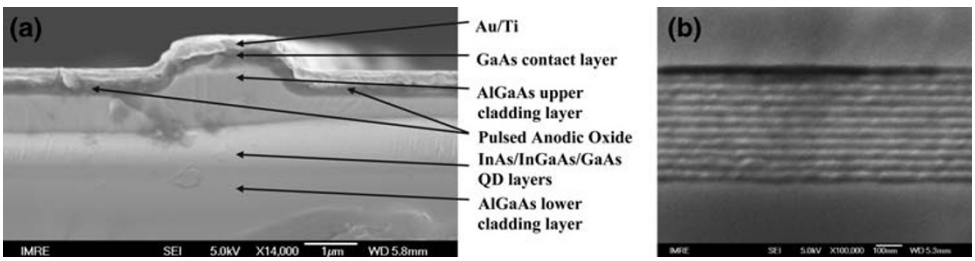

Fig. 2 (**a**) Cross-sectional SEM image of the InAs QD laser fabricated using PAO. (**b**) SEM image of the ten-stacked InAs QD layers for the same device as in (**a**)

gain, which consequently changes the oscillation wavelength as well as output power.

The unstable switching between modes causes intensity noise, resulting in degradation in the laser performance [31]. Furthermore, mode hopping is expected to be more pronounced in narrow ridge structures where the cross-sectional area is relatively small. More detailed investigation on the mode hopping behavior is warranted to further study this effect. Nevertheless, our observations from operating the device in CW mode suggest the presence of a significant heating effect.

To alleviate the effects of device heating in CW operation, the InAs QD lasers were measured under pulsed operation (1 μs, duty cycle = 1%) at 20 °C. Figure 4 shows the output power–current characteristics for a $2 \times 2{,}000$ μm^2 device with uncoated facets. Extremely high output power of 610 mW (per facet) was recorded at injection current of 1.6 A. To the best of our knowledge, this is among the highest value of output power in the literature ever reported for narrow RWG InAs QD lasers. Compared with CW operation, power saturation and kinks in the output power characteristics are greatly reduced in pulsed mode, which is attributed to reduction in device heating. High slope efficiency η of 0.46 W A^{-1} per facet was obtained from the *P–I* curve, and near ideal external differential quantum efficiency η_d of 96% was calculated from Eq. 1 [32]:

$$\eta_d = 2 \times \frac{\Delta P/\Delta(h\nu)}{\Delta I/\Delta q} = 2 \times \frac{\Delta P}{\Delta I} \times \frac{\lambda\ (\mu m)}{1.24\ (eV)} \qquad (1)$$

where η_d is the external differential quantum efficiency of the InAs QD laser, and $\Delta P/\Delta I$ is the slope efficiency obtained from the measured *P–I* characteristics. h is the Planck's constant, q the electronic charge, frequency $\nu = \frac{c}{\lambda}$, where c is the speed of light in vacuum, and λ the emission wavelength of the InAs QD laser. The far-field patterns (FFP) shown in the inset of Fig. 4 indicate the InAs RWG QD laser emitted at single lateral mode under different injection current levels from 450 mA to 600 mA. The laser beam divergence in the lateral direction is around 4° at the injection current levels investigated, indicating excellent beam quality in these devices.

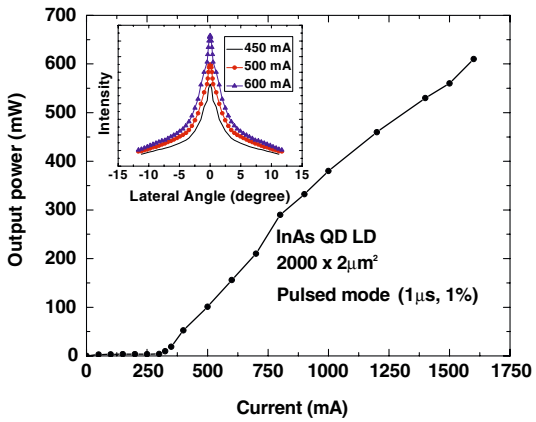

Fig. 4 *P–I* characteristics of a $2 \times 2{,}000$ μm^2 RWG InAs QD laser in pulsed operation (1μs, duty cycle = 1%) at 20 °C. Inset shows the lateral far-field pattern at different injection current levels in pulsed mode (1 μs, duty cycle = 1%) at 20 °C

Ouyang et al. [15] has reported narrow RWG InAs QD lasers with ridge width of 8 μm, and observed that lasers with deep-mesa geometry exhibited superior characteristics compared with shallow-mesa devices. Under pulsed operation (500 ns, 5 kHz), the HR/uncoated InAs QD laser of dimension $8 \times 1{,}500$ μm^2 showed high external differential efficiency of 50% and low threshold current density of ~130 A/cm^2 at moderate output power ~6 mW. Compared with this report, our results show that the ten-layer InAs QD lasers fabricated using PAO were able to deliver comparable, and in some cases better performance with near ideal external differential efficiency of 96% and extremely high output power of 610 mW/facet under pulsed operation. Furthermore, the devices also exhibit single lateral mode emission.

The output power P and external differential quantum efficiency η_d of our ten-layer InAs narrow RWG QD lasers are among the highest values in the 1.29–1.30 μm wavelength range ever reported. The high device performance is attributed to the high quality QD laser structure and optimized self-aligned PAO method compared with conventional SiO_2 confinement. The better passivation of the sidewalls by the native oxide formed by the PAO process could contribute to the reduction in nonradiative centers between the sidewall and oxide layer. This is particularly critical in narrow RWG devices such as the ones investigated in this study. These factors are believed to have contributed significantly to the high performance observed in our narrow RWG devices.

Conclusions

In summary, narrow RWG lasers based on ten-layer InAs/InGaAs QD active region have been fabricated and characterized. Devices fabricated using an optimized PAO process exhibited GS lasing at high total output power of 272.6 mW at ~1.3 μm under CW operation. Extremely high single lateral mode output power of 610 mW/facet was achieved in pulsed operation with minimal power saturation under high current injection. High slope efficiency of 0.46 W A^{-1} per facet, near ideal external differential quantum efficiency of 96% and low lateral beam divergence of 4° have been achieved in the devices.

Acknowledgements This research is partially sponsored by A*STAR under the ONFIG-II program SERC Grant No. 042 108 0098. The authors would also like to acknowledge the assistance of Dr Tong Cunzhu for his useful inputs to this research.

References

1. S.F. Yoon, C.Y. Liu, Z.Z. Sun, K.C. Yew, Nanoscale Res. Lett. **1**, 20 (2006)
2. S. Mokkapati, M. Buda, H.H. Tan, C. Jagadish, Appl. Phys. Lett. **88**, 161121 (2006)
3. S.S. Mikhrin, A.R. Kovsh, I.L. Krestnikov, A.V. Kozhukohov, D.A. Livshits, N.N. Ledentsov, Yu.M. Shernyakov, I.I. Novikov, M.V. Maximov, V.M. Ustinov, Zh.I. Alferov, Semicond. Sci. Technol. **20**, 340 (2005)
4. Y.H. Chen, X.L. Ye, Z.G. Wang, Nanoscale Res. Lett. **1**, 79 (2006)
5. O.B. Shchekin, D.G. Deppe, IEEE Photon. Technol. Lett. **14**, 1231 (2002)
6. A.R. Kovsh, N.A. Maleev, A.E. Zhukov, S.S. Mikhrin, A.P. Vasil'ev, Yu.M. Shernyakov, M.V. Maximov. D.A. Livshits. V.M. Ustinov, Zh.I. Alferov, N.N. Ledentsov, D. Bimberg, Electron. Lett. **38**, 1104 (2002)
7. O.G. Schmidt, N. Kirstaedter, N.N. Ledentsov, M.H. Mao, D. Bimberg, V.M. Ustinov, A.Y. Egorov, A.E. Zhukov, M.V. Maximov, P.S. Kop'ev, Z.I. Alferov Electron. Lett. **32**, 1302 (1996)
8. C.Y. Liu, S.F. Yoon, Q. Cao, C.Z. Tong, Z.Z. Sun, Nanotechnology **17**, 5627 (2006)
9. H.Y. Liu, D.T. Childs, T.J. Badcock, K.M. Groom, I.R. Sellers, M. Hopkinson, R.A. Hogg, D.J. Robbins, D.J. Mowbray, M.S. Skolnick, IEEE Photonics Technol. Lett. **17**, 1139 (2005)
10. M. Benyoucef, A. Rastelli, O.G. Schmidt, S.M. Ulrich, P. Michler, Nanoscale Res. Lett. **1**, 172 (2006)
11. L.V. Asryan, Appl. Phys. Lett. **88**, 073107 (2006)
12. M.V. Maximov, Yu.M. Shernyakov, I.N. Kaiander, D.A. Bedarev, E.Yu. Kondrat'eva, P.S. kop'ev, A.R. Kovsh, N.A. Maleev, S.S. Mikhrin, A.F. Tsatsul'nikov, V.M. Ustinov, B.V. Volovik, A.E. Zhukov, Zh.J. Alferov, N.N. Ledentsov, D. Bimberg, Electron. Lett. **35**, 2038 (1999)
13. S.S. Mikhrin, A.E. Zhukov A.R. Kovsh, N.A. Maleev, V.M. Ustinov, Yu.M. Shernyakov, I.N. Kayander, E.Yu. Kondrat'eva, D.A. Livshits, I.S. Tarasov, M.V. Maksimov, A.F. Tsatsul'nikov, N.N. Ledentsov, P.S. Kop'ev D. Bimberg, Zh.I. Alferov, Semiconductors **34**, 119 (2000)
14. C.Y. Liu, S.F. Yoon, Q. Cao, C.Z. Tong, H.F. Li, Appl. Phys. Lett. **90**, 041103 (2007)
15. D. Ouyang, N.N. Ledentsov, D. Bimberg, A.R. Kovsh. A.E. Zhukov, S.S. Mikhrin, V.M. Ustinov, Semicond. Sci. Technol. **18**, L53 (2003)
16. A.E. Zhukov, A.R. Kovsh, D.A. Livshits, V.M. Ustinov, Zh.I. Alferov, Semicond. Sci. Technol. **18**, 774 (2003)
17. A. Markus, J.X. Chen, C. Paranthoen, A. Fiore, C. Platz, O. Gauthier-Lafaye, Appl. Phys. Lett. **82**, 1818 (2003)
18. A.R. Kovsh, J.S. Wang, R.S. Hsiao, L.P. Chen, D.A. Livshits, G. Lin, V.M. Ustinov, J.Y. Chi, Electron. Lett. **39**, 1726 (2003)
19. C.S. Peng, N. Laine, J. Konttinen, S. Karirnne, T. Jouhti, M. Pessa, Electron. Lett. **40**, 604 (2004)
20. N. Tansu, J.Y. Yeh, L.J. Mawst, J. Phys.: Condens. Matter. **16**, S3277 (2004)
21. A. Caliman, A. Ramdane, D. Meichenin, L. Manin. B. Sermage, G. Ungaro, L. Travers, J.C. Harmand, Electron. Lett. **38**, 710 (2002)
22. M. Legge, G. Bacher, S. Bader, A. Forchel, H.-J. Lugauer, A. Waag, G. Landwehr, IEEE Photon. Technol. Lett. **12**, 236 (2000)
23. S.Y. Hu, D.B. Young, A.C. Gossard, L.A. Coldren, IEEE J. Quantum Electron. **30**, 2245 (1994)
24. D. Ban, E.H. Sargent, K. Hinzer, St. Dixon-Warren, A.J. SpringThorpe, J.K. White, Appl. Phys. Lett. **82**, 4166 (2003)
25. S. Slivken, J.S. Yu, A. Evans, J. David, L. Doris, M. Razeghi, IEEE Photon. Technol. **16**, 1041 (2004)
26. C.Y. Liu, Y. Qu, S. Yuan, S.F. Yoon, Appl. Phys. Lett. **85**, 4594 (2004)
27. C.Y. Liu, S.F. Yoon, S.Z. Wang, S. Yuan, J.R. Dong, J.H. Teng, S.J. Chua, IEE Proc. Optoelectron. **152**, 205 (2005)
28. X.D. Huang, A. Stintz, C.P. Hains, G.T. Liu, J.L. Cheng, K.J. Malloy, IEEE Photon. Technol. Lett. **12**, 227 (2000)
29. C.Y. Liu, S.F. Yoon, W.J. Fan. A. Uddin, S. Yuan, IEEE Photon. Technol. Lett. **18**, 791 (2006)
30. S. Yuan, C. Jagadish, Y. Kim, Y. Yang, H.H. Tan, R.M. Cohen, M. Petravic, L.V. Dao, M. Gal, M.C.Y. Chan, E.H. Li, S.O. Jeong, P.S. Zory Jr., IEEE J. Select. Topics Quantum Electron. **4**, 629 (1998)
31. M.F.C. Schemmann, C.J. van der Poel, B.A.H. van Bakel, H.P.M.M. Ambrosius, A. Valster, J.A.M. van den Heijkant, G.A. Acket, Appl. Phys. Lett. **66**, 920 (1995)
32. V.M. Ustinov, A.E. Zhukov, A.Y. Egorov, N.A. Maleev, *Quantum Dot Lasers*. (Oxford University Press, 2003)